



# Disordering kinetics of Ni<sub>3</sub>Al under ion irradiation

S. Müller<sup>a</sup>, C. Abromeit<sup>a,\*</sup>, S. Matsumura<sup>b</sup>, N. Wanderka<sup>a</sup>, H. Wollenberger<sup>a</sup>

<sup>a</sup> *Hahn-Meitner-Institut Berlin, Glienicker Str. 100, D-14109 Berlin, Germany*

<sup>b</sup> *Department of Nuclear Engineering, Kyushu University 36, Fukuoka 812-81, Japan*

## Abstract

The stability of the long-range-ordered (LRO)  $\gamma'$  phase was investigated in the temperature interval  $100 \text{ K} \leq T \leq 773 \text{ K}$  under 300 keV Ni<sup>+</sup> irradiation. The radiation-induced intensity changes of the L1<sub>2</sub> superlattice reflections were monitored by TEM technique using a computer assisted, quantitative evaluation of the amplitudes of diffraction patterns obtained by image plates. The dynamical diffraction theory where the thickness of the investigated foils was taken into account was employed to determine the degree of order from the diffraction patterns. The fluences were varied up to 10 dpa. The results are compared with recent measurements of disordered zone sizes after low dose ion irradiation in Ni<sub>3</sub>Al. The measured temperature dependence below room temperature is consistent with the predictions of the thermal spike model for disordering, but for higher temperatures the results hint to a more complicated re-ordering process in disordered areas. A Ni<sub>3</sub>Al specimen which was completely disordered after 10 dpa at 200 K was used for a thermal annealing experiment. The annealing behavior confirms the importance of the heterogeneous state of the order for the re-ordering process under ion irradiation. © 1999 Published by Elsevier Science B.V. All rights reserved.

## 1. Introduction

Nickel base alloys as for instance Nimonic PE16 or In738LC contain fine particles of the ordered  $\gamma'$  phase Ni<sub>3</sub>(Al,Ti). The  $\gamma'$  precipitates are the main hardening components in these alloys. However ordered alloy phases at temperatures below the critical order–disorder temperature  $T_c$  can be chemically disordered or/and amorphised by external forcing. An example is the destruction of the order in long-range-ordered (LRO) alloys by ball milling [1], cold work [2] or irradiation with energetic particles such as electrons, ions or neutrons [3]. With the loss of the ordered phase the mechanical properties of the materials will be deteriorated [4,5]. Therefore the disordering kinetics of the ordered  $\gamma'$  phase under external forces is of big interest and was studied in the present paper for Ni<sub>3</sub>Al in the temperature interval  $100 \text{ K} \leq T \leq 773 \text{ K}$  under 300 keV Ni<sup>+</sup> irradiation.

For irradiation temperatures below  $T_c$  partial re-ordering may occur. The thermal re-ordering was studied

by means of annealing of a disorder Ni<sub>3</sub>Al specimen irradiated at 200 K up to 100 dpa. The results are compared with those obtained for disordered Ni<sub>3</sub>Al produced by cold working or evaporation.

## 2. Experimental

Ni<sub>3</sub>Al single crystals supplied by MaTek, Jülich, Germany were used in the present investigation. Thin discs of 0.7 mm thickness were cut from the single crystals and mechanically polished down to 0.2 mm thick foils. Discs with 3 mm diameter suitable for transmission electron microscopy (TEM) investigations were punched out of these foils. For irradiation, these specimens were electrochemically polished from one side at 263 K in a TENUPOLE electropolishing unit using an electrolyte of 10% perchloric acid and 90% isopropyl alcohol at a voltage of 15 V. After irradiation the specimens were electrochemically thinned from the non-irradiated side until perforation occurred.

The TEM specimens were irradiated with 300 keV Ni<sup>+</sup> ions at a temperature between 100 and 773 K by using the SIB accelerator at the Hahn-Meitner-Institut, Berlin. The displacement cross section  $\sigma_d$  was computed

\* Corresponding author. Tel.: +49-30 8062 2825; fax: +49-30 8062 3059; e-mail: abromeit@hmi.de

by using the TRIM code [6] with the modified Kinchin-Pease expression with a displacement energy of 40 eV [7]. The displacement cross section depends on depth from the surface but does not deviate by more than 30% from its mean value  $\sigma_d = 1.6 \times 10^{-19} \text{ m}^2$  within 100 nm below the surface. The specimens were irradiated with a constant flux density  $\varphi = 1.6 \times 10^{16} \text{ m}^{-2} \text{ s}^{-1}$ . The corresponding displacement rate  $K = \varphi \sigma_d$  amounted to  $2.5 \times 10^{-3} \text{ dpa s}^{-1}$ . The irradiation was performed up to fluences of 10 dpa.

The ordering kinetics was studied using a sample which was disordered by 300 keV  $\text{Ni}^+$  irradiation at 200 K up to 10 dpa with subsequent annealing for 60 min at various temperatures. The specimens were examined in a Phillips EM400 electron microscope operating at 100 kV.

### 3. Determination of the state of order by TEM

Disordering and subsequent re-ordering of the  $\text{L1}_2$  structure of  $\text{Ni}_3\text{Al}$  is investigated by means of transmission electron microscopy. From the intensities of the selected area diffraction superlattice reflections, the average degree of the order in the alloy can be determined. Local variations of the ordered state are not resolved by this method.

In most cases, the degree of order, i.e. the long-range order parameter  $S$  is calculated by means of the kinematical diffraction theory according to  $S \sim \sqrt{I_{\text{SLR}}/I_{\text{FR}}}$ , where  $I_{\text{SLR}}$  and  $I_{\text{FR}}$  are the intensities of the superlattice reflections and fundamental reflections, respectively [8].

In the case of electron diffraction the intensity change due to the interference of the excited reflections is so significant that the kinematical approximation should break down [9]. Therefore we have used the dynamical diffraction theory for determination of  $S$ . The difference between the two approaches is demonstrated in Fig. 1, where for the exact  $[001]$  orientation the calculated intensity ratios of the  $(110)$  and  $(220)$  reflections are shown as the function of the order parameter  $S$  for various sample thicknesses. The vertical axis represents the intensity ratio between the  $[110]$  super-reflection with respect to the fundamental reflection. The intensities are symmetrical with respect to the transmitted beam. They were calculated with the EMS-Software [10]. The relationship between  $S$  and  $I_{\text{SLR}}/I_{\text{FR}}$  depends sensitively on the sample thickness. Only for very thin samples  $S$  as a function of  $I_{\text{SLR}}/I_{\text{FR}}$  can be described by a quadratic dependency as it is given by the kinematical theory. For thicker samples the dynamical diffraction effect becomes significant, and the relationship of  $S$  and  $I_{\text{SLR}}/I_{\text{FR}}$  considerably deviates from the prediction by the kinematical approximation. For some cases i.e. for the foil thicknesses of 14 and 46 nm the dynamical diffrac-

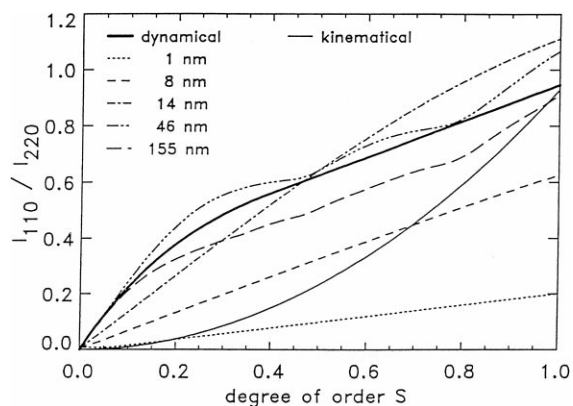


Fig. 1. Intensity ratios  $I_{110}/I_{220}$  versus order  $S$  parameter  $S$  for various sample thicknesses calculated within the dynamical theory (broken lines). Bold Line: approximated relationship which is used for the determination of  $S$  from measured intensity ratios. Full thin line: results of kinematical theory for comparison.

tion effect even causes an intensity ratio  $I_{\text{SLR}} > I_{\text{FR}}$  for highly ordered alloys ( $S \sim 1$ ). As the samples in the present study were thicker than 45 nm, we utilized the average averaged relationship between  $S$  and  $I_{\text{SLR}}/I_{\text{FR}}$  derived on the dynamical diffraction theory, which is delineated in a solid line in Fig. 2. The maximum error of about 40% results from the neglect of the details of the thickness dependence for samples thicker than 45 nm. Similar relationships have been found for the intensity ratios of the  $(100)$  and  $(200)$  reflections [11].

The intensities of the reflections by TEM are measured by image plates (FUJI), which are digitized by the FUJI scanners 'BAS 1000' and 'FDL 5000' [12]. An

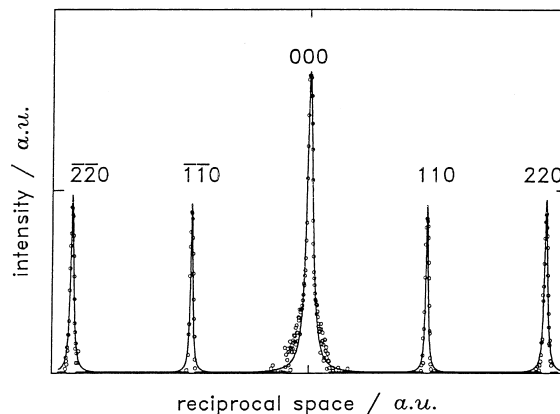


Fig. 2. Measured intensity profiles for the  $[001]$  zone axis case of  $\text{Ni}_3\text{Al}$  reflections after 300 keV  $\text{Ni}^+$  irradiation at 200 K up to a fluence of 0.01 dpa. The fit by Lorentzian shape functions is also shown.

example of an intensity profile for the exactly oriented  $[0\ 0\ 1]$  zone axis is shown in Fig. 2. It was taken from an  $\text{Ni}_3\text{Al}$  sample which was irradiated with 300 keV  $\text{Ni}^+$  ions at a temperature  $T=200$  K up to a fluence of 0.01 dpa. The profiles were fitted by Lorentz functions for the determination of the amplitudes of the intensities  $I_{\text{SLR}}$  and  $I_{\text{FR}}$ .

## 4. Results and discussion

### 4.1. Disorder kinetics of LRO ordered $\text{Ni}_3\text{Al}$

The results of the disordering of initially ordered  $\text{Ni}_3\text{Al}$  by 300 keV  $\text{Ni}^+$  are shown in Fig. 3. The order parameter  $S$  was calculated from the measured intensity ratios by the relationship as given in Fig. 1. The temperature dependence of the kinetics displayed in Fig. 3 shows that the order is most efficiently destroyed at room temperature (RT). At temperatures below RT, the completely disordered state is obtained after a fluence larger than 1 dpa. At temperatures above RT, a given degree of disorder needs increasing fluences with increasing irradiation temperature. It should be noted that cascade production is connected with the formation of extended defect clusters. They have been studied in detail in  $\text{Ni}_3\text{Al}$  for very small fluences i.e. for the highly ordered state [13].

The experimental results are in general accordance with earlier qualitative observations under the similar irradiation conditions [14]. However, due to the improved data evaluation, the present data allow a quantitative discussion based on a modified thermal spike model for the state of order in alloys under cascade producing irradiation [11]. The thermal spike model assumes that inside a cascade a thermal spike evolves in

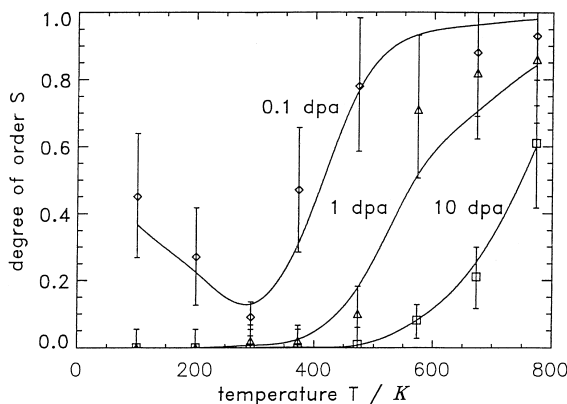


Fig. 3. Disorder kinetics of initially ordered  $\text{Ni}_3\text{Al}$  by 399 keV  $\text{Ni}^+$  irradiation for various temperatures and fluences. The curves are fits according to the modified thermal spike model with an efficiency function  $\kappa(t, T)$  as shown in Fig. 4.

time due to the energy dissipation to its environment. During the evolution of the thermal spike there are a heating and a cooling phase. At the end of the heating phase the disordered zones produced by the thermal spike expand to the maximum extension  $V_{\text{max}}$ . During the following cooling phase some re-ordering may occur.

At very low sample temperatures the deposited energy dissipates into the matrix quickly. The maximum extension of the disordered zone with the volume  $V_{\text{max}}$  is assumed to be frozen in. With increasing temperatures the cooling rate becomes smaller and a larger volume is heated by the locally deposited thermal spike. The maximum disordered volume  $V_{\text{max}}$  increases with temperature in agreement with the experimental results reported by Bui et al. [15]. It indicates that the re-ordering during the following cooling phase is negligible so that the disordered state inside the cascade volume is conserved. As the disordering efficiency  $\varepsilon$  for low temperature irradiations is proportional to the disordered volume  $\varepsilon = -\ln(S(t)/S(t=0))/Kt \sim V_{\text{max}}$ , the disordering efficiency increases with increasing temperature. This behavior is obviously valid up to RT.

Above RT, re-ordering of disordered zones during the cooling phase of the thermal spike may be no more neglected. This process reduces the maximum disordered volume  $V_{\text{max}}$  to a smaller disordered volume  $V_d$ . In the simple thermal spike approach [16] the re-ordering is assumed to be the same whether the cascades are produced in an ordered region or in an already disordered region. Then, the average degree of order reaches a stationary value for long irradiation times  $S_{\infty}(T) = 1 - V_d/V_{\text{max}}$  which depends only on the ratio of the disordered volume  $V_d$  after the cooling phase of the cascade evolution to the maximum disordered volume  $V_{\text{max}}$ . However, a fit to the experimental data is not possible by means of realistic parameters. The reordering process seems to become less efficient for high irradiation fluences, i.e. for smaller degrees of order. Such behavior was observed also for conventional thermal annealing of disordered states [17,18]. In the modified thermal spike model [11], the disordering kinetics is approximated by

$$\frac{\partial S}{\partial t} = -\varepsilon KS + \kappa(t, T) \left( \varepsilon KS_{\infty}(T) + \left( \frac{\partial S}{\partial t} \right)_{\text{th}} \right), \quad (1)$$

where  $\kappa = \kappa(t, T)$  is a modification factor for the reduced re-ordering after higher fluences. The third term of Eq. (1) describes the irradiation enhanced thermal re-ordering by migrating point defects. It is important for higher temperatures and is taken into account by using an approach given by Banerjee and Urban [17]. The fit of Eq. (1) to the experimental data is also shown in the Fig. 3. The corresponding efficiency  $\kappa(t, T)$  is given in Fig. 4. It shows that the re-ordering is strongly reduced with increasing fluence.

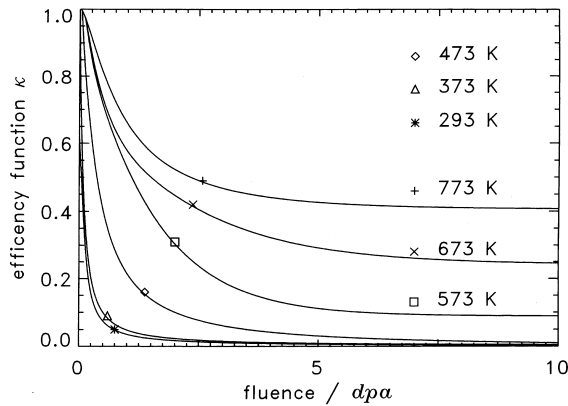


Fig. 4. Fitted efficiency function for re-ordering  $\kappa(t, T)$  versus irradiation fluence according to the modified thermal spike model (see Fig. 3).

#### 4.2. Re-ordering after heterogeneous disordering by irradiation

The re-ordering process is investigated by an annealing of disordered  $\text{Ni}_3\text{Al}$  specimen prepared by 10 dpa irradiation at 200 K. The sample was isochronally annealed between 273 and 873 K by steps of 50 K with the annealing period of 60 min. The intensity ratios are given in Fig. 5. Very weak intensities could be already detected after annealing at 373 and 473 K, which may be attributed to some short-range ordering. The same conclusion was drawn from DSC measurements of  $\text{Ni}_3\text{Al}$  disordered by ball milling [1]. This interpretation is consistent with the broad intensity profiles of the (1 1 0) superlattice reflections measured at these temperatures. For temperatures above 523 K the intensity profiles become sharp indicating the formation of the long-range ordered state (see Fig. 6).

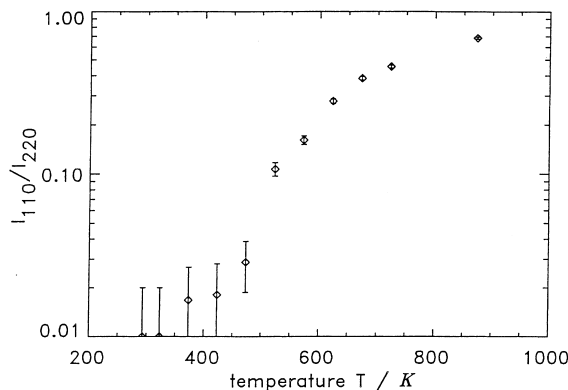


Fig. 5. Intensity ratios  $I_{110}/I_{220}$  versus annealing temperature of  $\text{Ni}_3\text{Al}$ , disordered with 300 keV  $\text{Ni}^+$  ion at 200 K after 10 dpa (annealing time: 60 min).

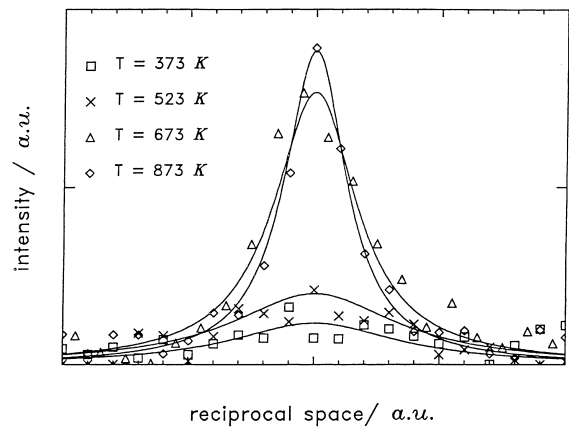


Fig. 6. Intensity profiles of the (1 1 0) superlattice reflection for the annealing temperatures 373 K, 523 K, 673 K and 873 K of  $\text{Ni}_3\text{Al}$ , disordered with 300 keV  $\text{Ni}^+$  ion at 200 K after 10 dpa (annealing time: 60 min).

It is interesting to note, that the transition of the disordered state to the LRO state occurs in a broad temperature interval from 373 to 873 K, which may be compared to the annealing behavior of disordered  $\text{Ni}_3\text{Al}$  obtained by evaporation of disordered layers [19] or by cold work treatment [2]. The former alloy exhibits a sharp transition from the disordered phase to the long-range order, while the latter case involves a broad transition accompanying the short-range ordering in a similar way as the irradiated alloy. Irradiation or cold work treatments create a heterogeneous microstructure consisting particularly of extended defect clusters etc. which are not produced by the evaporation technique. Extended defect structures obviously restrain the re-ordering process.

## 5. Conclusion

The destruction of an LRO structure under cascade producing irradiation has been investigated by means of the TEM technique using an improved data acquisition and interpretation which includes the following.

1. Computer assisted monitoring of the intensity changes of the reflection spots by imaging plates.
2. Calculation of the average state of order from the reflection intensities using the dynamical diffraction theory.

The experimental results can be successfully interpreted by:

1. A disordering kinetics due to thermal spikes in cascades.
2. Simultaneous disordering and re-ordering processes at elevated temperatures.

3. An annealing behavior of the heterogeneous disordered state which significantly differs from the homogeneous state.

### References

- [1] M.D. Baro, S. Surinach, J. Malagelada, M.T. Clavaguera-Mora, S. Gialanella, R.W. Cahn, *Acta Metall. Mater.* 41 (1993) 1065.
- [2] R. Kozubski, M. Migschitz, W. Pfeiler, in: A. Gonis et al. (Eds.), *Stability of Materials*, Plenum, New York, 1996, p. 699.
- [3] E.M. Schulson, *J. Nucl. Mater.* 83 (1979) 239.
- [4] E. Nembach, G. Neite, *Prog. Mater. Sci.* 29 (1985) 177.
- [5] F. Bourdeau, E. Camus, C. Abromeit, H. Wollenberger, *Phys. Rev. B* 50 (1994) 16205.
- [6] J.P. Biersack, L.G. Haggmark, *J. Nucl. Instr. Meth.* 174 (1980) 257.
- [7] F. Gao, D.J. Bacon, *Philos. Mag. A* 71 (1995) 43.
- [8] G.J.C. Carpenter, E.M. Schulson, *Scripta Metall.* 15 (1981) 549.
- [9] K. Urban, *Phys. Stat. Sol. A* 87 (1985) 459.
- [10] P.A. Stadelmann, *Ultramicroscopy* 21 (1987) 131.
- [11] S. Müller, Thesis D 83, TU Berlin, 1997.
- [12] S. Baba, H. Kimata, S. Haruki, Y. Shinohara, *Appl. Radiat. Iso.* 7 (1993) 1011.
- [13] S. Müller, M.L. Jenkins, C. Abromeit, H. Wollenberger, *Philos. Mag. A* 75 (1997) 1625.
- [14] C. Abromeit, S. Müller, N. Wanderka, *Scripta Metall. Mater.* 32 (1995) 1519.
- [15] T.X. Bui, I.M. Robertson, M.A. Kirk, *Mater. Res. Soc. Symp. Proc.* 373 (1995) 63.
- [16] C. Abromeit, H. Wollenberger, *J. Nucl. Mater.* 191–194 (1992) 1092.
- [17] S. Banerjee, K. Urban, *Phys. Stat. Sol. (a)* 81 (1984) 145.
- [18] R.H. Zee, P. Wilkes, *Philos. Mag. A* 42 (1986) 878.
- [19] S.R. Harris, D.H. Pearson, C.M. Garland, B. Fultz, *J. Mater. Res.* 6 (1991) 2019.